Low-frequency Noise Characterization of Graphene FET THz Detectors

Low-frequency Noise Characterization of Graphene FET THz Detectors

Xinxin Yang[1], Andrei Vorobiev[1], Kjell Jeppson[1], Jan Stake[1], Luca Banszerus[2], Christoph Stampfer[2], Martin Otto[3] and Daniel Neumaier[3]

[1]Chalmers University of Technology, SE-41296 Gothenburg, Sweden

[2]RWTH Aachen University, DE-52074 Aachen, Germany

[3]AMO GmbH, DE-52074 Aachen, Germany

***Abstract*—Graphene field-effect transistors are promising for direct detection of THz signals at room temperature. The sensitivity of such detectors can be in part limited by the low-frequency noise. Here, we report on the characterization of the low-frequency noise of graphene field-effect transistor THz detectors in the frequency range from 1 Hz to 1 MHz. The room-temperature Hooge parameter is extracted to be around 2×10^{-3}. The voltage responsivity at room-temperature and the corresponding minimum noise equivalent power at 0.3 THz are estimated to be 11 V/W and 0.2 nW/Hz$^{0.5}$, respectively, at a modulation frequency of 333 Hz, which shows comparable results with other detector technologies.**

I. Introduction

GRAPHENE, with its high carrier mobility and saturation velocity, is a promising material for high-frequency devices. In recent years, room-temperature THz detectors based on graphene field-effect transistors (GFETs) have been demonstrated [1, 2]. An important figure of merit of direct power detectors is the noise equivalent power (NEP), which corresponds to the lowest detectable power [3]. Most of previous studies have estimated the NEP of GFET THz detectors based on responsivity measurements and thermal noise calculations. Assuming a short integration time, the low-frequency noise can be avoided. However, impurities and other defects introduced during the fabrication process are expected to contribute to the low-frequency noise [4, 5], and thereby degrade the detector performance. It is important to understand the noise spectrum for detector applications. In this work, we have characterized the low-frequency noise in GFET THz detectors. This allows us to find a low frequency limit of the modulation frequency, above which the low-frequency noise is negligible.

II. Results

GFET THz detectors were fabricated using monolayer CVD graphene made by RWTH and AMO as in [2]. Fig. 1 shows an optical micrograph and a schematic cross-sectional view of a GFET THz detector with a mesa length (L) of 0.7 µm, a gate length of 0.5 µm and an effective channel width (W) of 20 µm (two 10-µm wide gates in parallel). The rectified THz voltage (V_{THz}) was measured on-wafer using Cascade T-Wave ground-signal-ground probes and an SR830 lock-in amplifier. The 0.3-THz input signal was modulated at 333 Hz. The THz source was composed of a WR-3.4 extender driven by an Agilent 8275D signal generator. The input THz power was around 80 µW considering of the insertion loss of the probes and the return loss of the detectors. The voltage noise spectral density ($S_{V,10mV}$) of the low-frequency noise was measured at room temperature using a Keysight E4727A Advanced Low-Frequency Noise Analyzer. During the experiment, the sample was placed inside a grounded metal box to minimize environmental noise. The drain-source voltage (V_{DS}) was set to 10 mV since limitations in the setup sensitivity make it hard to measure the noise level with the same drain bias as low as V_{THz}. The gate leakage current was less than 0.6 nA posing only negligible effects on the noise level.

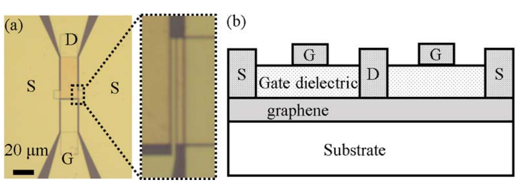

Fig. 1. Optical micrograph (a) and schematic cross-sectional view (b) of a GFET THz detector with a gate length of 0.5 µm, and an effective channel width of 20 µm (two 10-µm wide gates in parallel).

Fig. 2 (a) shows the measured drain-source resistance (r_{DS}) of a typical GFET THz detector plotted versus the gate voltage (V_{GS}). By fitting the measured resistance to the model described in [6], the electron mobility, the residual carrier concentration, and the contact resistance were extracted to be 2000 cm^2/Vs, 1.7×10^{12} cm^{-2}, and 22 Ω, respectively. The charge carrier concentration (n) was estimated to be in the range from 1.7×10^{12} to 5.5×10^{12} cm^{-2}. Fig. 2 (b) shows the rectified THz voltage as a function of V_{GS}. The rectified THz voltage is in the range from 0.04 to 0.16 mV.

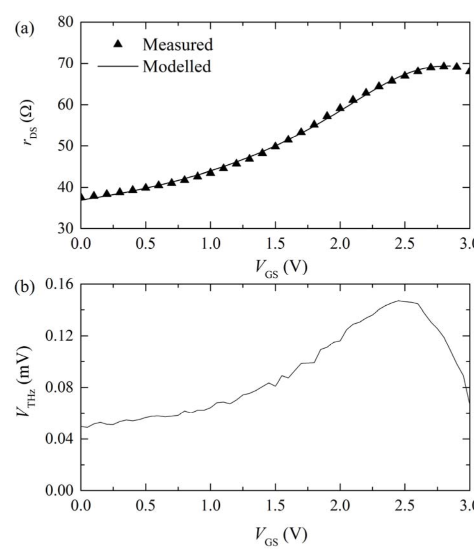

Fig. 2. (a) The measured drain-source resistance of the detector as a function of V_{GS} (symbols), together with the fitting result (solid line). (b) The measured rectified THz voltage of the detector as a function of V_{GS} without drain-source bias at 0.3 THz.

978-1-5386-3809-5/18/$31.00 ©2018 IEEE

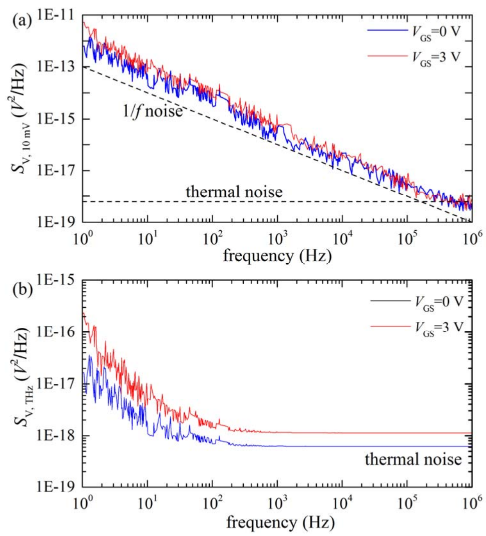

Fig. 3. (a) Measured noise spectral density of the detector vs. V_{GS} at V_{DS}=10 mV. (b) Calculated noise spectral density of the detector vs. V_{GS} at V_{DS}= V_{THz}.

Fig. 3 (a) shows the noise spectral density of the detector measured at two different gate voltages together with the thermal noise calculated as in [1]. It can be seen that the noise spectral density reveals a 1/*f* dependence. The observed 1/*f* noise is caused by low-frequency fluctuations of the channel resistance due to fluctuations in carrier concentration and/or mobility [4, 5]. The 1/*f* noise ($S_{V,1/f}$) at a 10 mV drain-source voltage can be estimated by subtracting the calculated thermal noise. Assuming negligible current-induced heating effects, the Hooge model [7] can be used to estimate the 1/*f* noise of the detector with a drain-source bias at V_{THz} from,

$$S_{V\mathrm{THz},1/f} = S_{V,1/f}\left(\frac{V_{\mathrm{THz}}}{V_{\mathrm{DS}}}\right)^2,$$

where V_{DS}=10 mV. The noise spectral density ($S_{V,\mathrm{THz}}$) at V_{THZ} can now be obtained by again adding the previously subtracted thermal noise as shown in Fig 3 (b). As shown by the graph, the total noise is defined mainly by the thermal noise at frequencies higher than 100 Hz. This means that we can eliminate the effects of the 1/*f* noise by using modulation frequencies higher than 100 Hz.

We can evaluate the Hooge parameter based on $S_{V,1/f}$ and the device parameters [7]

$$\alpha_{\mathrm{H}} = \frac{S_{V,1/f}}{V_{\mathrm{DS}}^2} * Nf \approx 2\times10^{-3},$$

where N=nWL is the number of carriers. α_{H} is 2~3 orders of magnitude larger than those of mature semiconductors [7].

Fig. 4 shows the room-temperature THz voltage responsivity (R_V) and the NEP, which are important figures of merit for the direct power detector. The voltage responsivity was calculated as in [2], and the NEP was obtained as NEP = $\sqrt{S_{V,\mathrm{THz}}}/R_V$. The maximum R_V is 11 V/W at V_{GS}=2.5 V, and the corresponding minimum NEP is 0.2 nW/Hz$^{0.5}$. The NEP is at the same level as other detector technologies, e.g. 0.65 nW/Hz$^{0.5}$ for silicon MOSFETs [8], 0.4 nW/Hz$^{0.5}$ for InP DHBTs [9] and 0.1 nW/Hz$^{0.5}$ for AlGaN/GaN HEMTs [10].

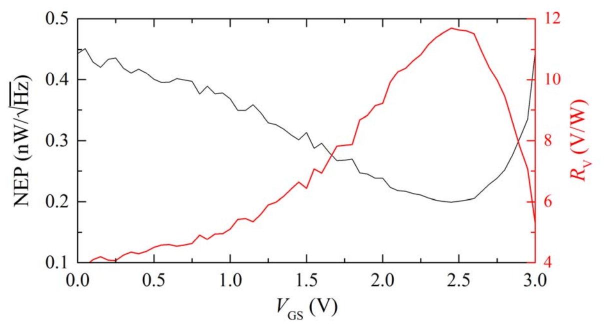

Fig. 4. NEP and voltage responsivity of the detector as a function of V_{GS} with a signal frequency of 0.3 THz.

III. SUMMARY

We have characterized the low-frequency noise of GFET THz detectors and found that modulation frequencies should be higher than 100 Hz to eliminate the effects of the 1/*f* noise. In this work, the Hooge parameter is around 2×10^{-3}, which is 2~3 orders of magnitude larger than those of mature semiconductors. The room-temperature responsivity and the corresponding minimum NEP at 0.3 THz were estimated to be 11 V/W and 0.2 nW/Hz$^{0.5}$, respectively. These values show the potential of GFET THz detector to compete with other detector technologies.

ACKNOWLEDGMENT

This work was supported in part by the EU Graphene Flagship Core 1 Project and in part by the Swedish Research Council (VR) under Grant No. 2017-04504.

REFERENCES

[1] L. Vicarelli et al., “Graphene field-effect transistors as room-temperature terahertz detectors,” *Nat. Mater.*, vol. 11, no. 10, pp. 865–871, 2012.

[2] A. A. Generalov et al., “A 400-GHz graphene FET detector,” *IEEE Trans. THz Sci. Technol.*, vol., vol. 7, no. 5, pp. 614–616, 2017.

[3] S. van Berkel et al., “THz imaging using uncooled wideband direct detection focal plane arrays,” *IEEE Trans. THz Sci. Technol.*, vol. 7, no. 5, pp. 481–492, 2017.

[4] A. A. Balandin, “Low-frequency 1/*f* noise in graphene devices,” *Nat. Nanotechnol.*, vol. 8, no. 8, pp. 549–555, 2013.

[5] A. Kaverzin, et al., “Impurities as a source of 1/*f* noise in graphene,” *Phys. Rev. B,* vol. 85, no. 7, p. 075435, 2012.

[6] S. Kim et al., “Realization of a high mobility dual-gated graphene field-effect transistor with Al_2O_3 dielectric,” *Appl. Phys. Lett.*, vol. 94, no. 6, p. 062107, 2009.

[7] J. Sikula et al., *Advanced experimental methods for noise research in nanoscale electronic devices*. Springer Science+Business Media, 2006, vol. 151.

[8] K. E. Seery et al., “Characterization of Si-MOSFET CMOS devices for detection at 170 to 250 GHz,” *SPIE OPTO*, San Francisco, United States, vol. 105311R, Jan. 27-Feb. 1, 2018.

[9] N. Dyakonova et al., “Reducing noise equivalent power in InP DHBT terahertz detector by biasing the collector,” *2017 ICNF*, pp. 1–4, Vilnius, Lithuania, Jun. 20-23, 2017.

[10] D. Čibiraitė et al, “Enhanced performance of AlGaN/GaN HEMT-based THz detectors at room temperature and at low temperature,” *2017 42nd IRMMW-THz*, pp. 1-2, Cancun, Mexico, Aug. 27-Sept. 1, 2017.